Scattering of Electromagnetic Wave By Bragg Reflector with Gyrotropic Layers

Alexander Shmat'ko[1](✉), Victoriya Mizernik[2], and E. Odarenko[3]

[1] School of Radiophysics, Biomedical Electronics and Computer Systems, V.N. Karazin Kharkiv National University, Kharkiv, Ukraine
alexandr.a.shmatko@univer.kharkov.ua
[2] Scientific Physical-Technologic Center of MES and NAS of Ukraine, Kharkiv, Ukraine
viknikm@ukr.net
[3] School of Electronics and Biomedical Engineering, Kharkiv National University of Radio Electronics, Kharkiv, Ukraine
yevhen.odarenko@nure.ua

Abstract. We solved the problem of scattering of plane wave on a ferrite 1D magnetophotonic crystal controlled by a dc transverse magnetic field. Fundamental solutions of the Hill equation with mixed boundary conditions based on the Floquet-Bloch theory are obtained in an analytical form. The dispersion equation and its roots are found explicitly. The analysis of the dispersion properties of the structures is carried out depending on the material parameters of the ferrite layers. The transmission and reflection coefficients are determined for the gyrotropic crystal with finite number of periods. Two characteristic cases are considered: positive and negative values of the effective permeability of gyrotropic layer. The expressions for spatial distribution of electromagnetic field components are determined at crystal period. The results provide a deeper understanding of the electromagnetic waves propagation behavior in multilayer media with controlled gyrotropic elements. In addition, the obtained analytical expressions simplify the analysis of wave processes in such complex media.

Keywords: Magnetophotonic crystal · Gyrotropic media · Hill's equation · Floquet-Bloch theory · Ferrite with dc transversal magnetic field · Dispersion characteristics · Band gap

1 Introduction

Magnetophotonic crystals (MPhC) are widely used in various applications of modern science and technology of the terahertz, microwave and optical ranges. Features of the transmission of electromagnetic waves through such structures are completely determined by the material parameters and the geometric dimensions of the layers. Dispersion properties of one-dimensional MPhC with isotropic layers are well studied, based on the obtained analytical characteristic equations for both TE and TM waves [1–8]. The most promising applications include MPhC in the presence of the gyrotropic of one or

© The Editor(s) (if applicable) and The Author(s), under exclusive license
to Springer Nature Switzerland AG 2021
M. Ilchenko et al. (Eds.): MCT 2019, LNNS 152, pp. 404–416, 2021.
https://doi.org/10.1007/978-3-030-58359-0_23

two layers of a periodic structure. The presence of gyrotropic layer in such structure makes it possible to change the values of the material parameters of the medium relatively easily due to the applied magnetic field and, as a result, to control the dispersion properties of the periodic structure and the wave transmission coefficient electrically. For gyrotropic MPhC there are no analytical expressions for the main frequency and amplitude characteristics of the scattered fields.

In the presence of gyrotropy the material parameters are tensor quantities. This is the main reason for necessity of obtaining an analytical solution for the problem of finding both the dispersion equation of a one-dimensional MPhC and the transmission and reflection coefficients of waves through an MPhC limited in the number of periods. In fact, the problem of scattering of a wave on the MPhC can be reduced to the study of the Hill equation with a discretely periodic medium. When solving the Hill equation, as a rule, the Floquet theory of waves [9–12] is used. Such problems were considered only for the case of isotropic two-layer discretely periodic media [13–23] where analytical expressions for the Floquet-Bloch functions in the layers were obtained. For gyrotropic MPhC, the Floquet theory approach was not considered.

In this paper, on the basis of the Floquet theory and the Hill equation, the problem of the scattering of plane wave on a bounded ferrite crystal with a controlling transverse magnetic field is solved analytically.

2 Floquet - Bloch Waves

Currently, MPhC are widely used in various devices for transmitting information in the terahertz range. To calculate the amplitude-frequency characteristics of such structures, the transfer matrix method [9–12, 14] is used usually. The most general case of calculating the dispersion characteristics in MPhC with bigirotropic layers using the transfer matrix method is given in [3, 6]. In this report, the problem of scattering of the E-polarization plane wave on a limited MPhC consisting of a finite number of periods of the ferrite and dielectric layers is considered. Scheme of structure under investigation and appropriate coordinate system are shown on Fig. 1. The problem is reduced to the Hill equation with variable coefficients, the solution of which is based on the Floquet theory. Let us turn to the solution of the problem.

We will consider the scattering of TM waves with a component of the magnetic field $H_z = 0$ $(H_x,\ H_y,\ E_z)$, E_z-polarization (s-polarization). Maxwell equations are reduced to the Helmholtz equation for the electric field component:

$$\frac{\partial}{\partial x}\left(\frac{1}{\mu_\perp(x)}\frac{\partial E_z}{\partial x}\right)+\frac{1}{\mu_\perp(x)}\frac{\partial^2 E_z}{\partial y^2}+k^2\varepsilon_j(x)E_z=0 \tag{1}$$

where $\mu_\perp(x)$ and $\varepsilon(x)$ are determined by the known formulas for the gyromagnetic ferrite layer and the dielectric layer [13], namely:

$$\overset{\leftrightarrow}{\mu}_j=\begin{Vmatrix}\mu_j & -i\mu_{aj} & 0\\ i\mu_{aj} & \mu_j & 0\\ 0 & 0 & \mu_{\|j}\end{Vmatrix},$$

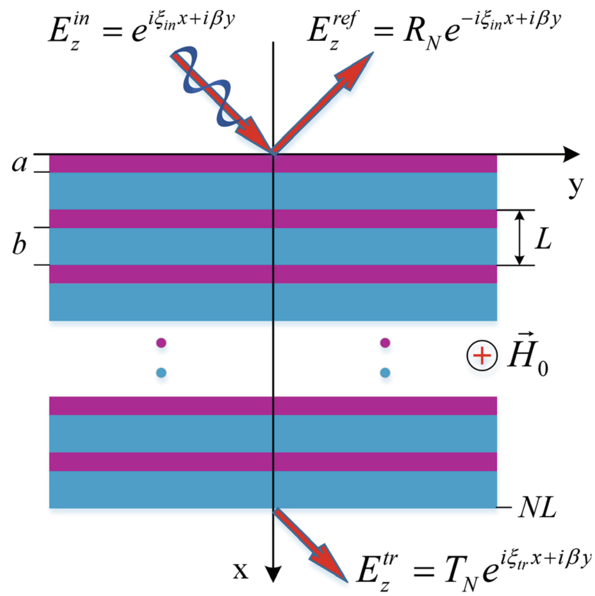

Fig. 1. Schematic of the ferrite Bragg structure.

where $\mu_{\perp j}(x) = \mu_j\left(1 - \mu_{aj}^2/\mu_j^2\right)$ is effective values of magnetic permeability of ferrite layers, $\varepsilon_j(x) = \varepsilon_j$ is dielectric constant of layers. Relationship between the field components H_y, E_z is determined by the expression:

$$H_y = -\left(\frac{1}{ik\mu_\perp}\right)\left(\frac{\partial E_z}{\partial x} + i\frac{\mu_a}{\mu}\frac{\partial E_z}{\partial y}\right). \tag{2}$$

It should be noted that the principle of permutation duality for the two types of waves (TM and TE) follows from Maxwell equations. Therefore it suffices to consider a single polarization of the waves. Solution for another polarization field (e.g. for H_z) is found by simply replacing the material parameters $\overset{\leftrightarrow}{\mu} \leftrightarrow -\overset{\leftrightarrow}{\varepsilon}$. All this allows us to simplify the consideration of a general electrodynamics problem and restrict ourselves to only one type of TE or TM wave for any type of medium. Equation (1) can be reduced by using the method of separation of variables $E_z(x, y) = X(x)e^{\beta y}$ to one kind of Hill equations with periodic coefficients, namely:

$$\frac{\partial}{\partial x}\left(p(x)\frac{\partial X}{\partial x}\right) + q(x)X = 0, \tag{3}$$

where $p(x)$ and $q(x)$ are periodic coefficients determined by expressions:

$$p(x) = \frac{1}{\mu_{\perp j}(x)},$$

$$q(x) = p(x)\left(k^2\varepsilon_j(x)\mu_{\perp j}(x) - \beta^2\right) = p(x)\xi^2(x) = p_j\xi_j^2$$

for TM waves. The value β determines the wave propagation constant along the axis $Oy(\exp(\pm i\beta y))$ and associated with the operator $\partial^2/\partial y^2 = -\beta^2$ in Helmholtz Eq. (1). We assume that the layout of the layers is as follows: a layer with an index $j = 1$ occupies areas of space $nL < x < a + nL$, layer with index $j = 2$ occupies additional area to the structure period $a + nL < x < L + nL$. Here $n = 0, 1, 2\ldots$ is period number.

The one-dimensional Eq. (3) is the Hill equation [9–12, 15–23] with periodic functions $p(x)$ and $q(x)$, such that $p(x + L) = p(x)$,$q(x + L) = q(x)$, where L is MPhC period. Equation (3) with the corresponding boundary conditions is the boundary Sturm-Liouville problem. According to Hill equation theory, if $\psi_1(x)$ is a particular solution of Eq. (3) with periodic coefficients then $\psi_1(x + L)$ is also solution. If $\psi_1(x)$ and $\psi_2(x)$ are two linearly independent solutions of Eq. (3) then $\psi_1(x + L)$ and $\psi_2(x + L)$ are also a solution of Hill equation. These solutions can be represented as a linear combination of two fundamental solutions $\psi_1(x)$ and $\psi_2(x)$, namely:

$$\left.\begin{array}{l}\psi_1(x+L) = a_{11}\psi_1(x) + a_{12}\psi_2(x)\\ \psi_2(x+L) = a_{21}\psi_1(x) + a_{22}\psi_2(x)\end{array}\right\}, \qquad (4)$$

where a_{nm} are constants to be defined. Therefore shift on the period L along coordinate axis Ox is reduced to linear combination of fundamental solutions $\psi_1(x)$ and $\psi_2(x)$. Two linearly independent fundamental solutions of Hill equation are chosen in such a way as to satisfy the boundary conditions:

$$\psi_1(0) = 1,\ \psi_1'(0) = 0,\quad \psi_2(0) = 0,\quad \psi_2'(0) = 1.$$

Using these boundary conditions for $\psi_1(x)$ and $\psi_2(x)$ constants in (4) can be obtained as follows: $a_{11} = \psi_1(L),\ a_{21} = \psi_2(L),\quad a_{12} = \psi_1'(L),\quad a_{22} = \psi_2'(L)$.

Then the characteristic equation for determining a Floquet constant ρ takes the standard form:

$$\rho^2 - 2A\rho + Wr(\psi_1, \psi_2) = 0, \qquad (5)$$

where

$$A = \frac{1}{2}\left[\psi_1(L) + \psi_2'(L)\right] = \cos\varphi,$$

$$Wr(\psi_1, \psi_2) = \psi_1(x)\psi_2'(x) - \psi_2(x)\psi_1'(x).$$

Naturally, in its meaning, the roots of the characteristic equation should not depend on the choice of fundamental solutions $\psi_1(x)$ and $\psi_2(x)$. Free term $Wr(\psi_1, \psi_2)$ in (5) is constant because it determines the Wronskian of the original equation. The introduction of the above boundary conditions to determine the fundamental solutions is connected with the well-known Dirichle and Neumann boundary value problems [15–23]. With regard to the MPhC with gyrotropic layers, such boundary conditions are not optimal from the point of view of the simplicity of finding the eigenfunctions of the Hill equation. In this case, to find fundamental solutions it is advisable to use mixed boundary conditions. This follows from the form of the field (2). Boundary conditions for finding solutions of Hill equation $X(x) = A\psi_1(x) + B\psi_2(x)$ connected to the continuity of the tangential field components on the boundaries of layers:

$$E_z(x, y) = X(x)e^{i\beta y}, \quad H_y(x, y) = \left(\frac{1}{-ik\mu_\perp}\right)\left(\frac{\partial X(x)}{\partial x} - \beta\frac{\mu_a}{\mu}X(x)\right),$$

and can be written as follows:

$$X_1(a) = X_2(a),$$

$$\frac{1}{\mu_{\perp 1}}\left(\frac{\partial X_1(a)}{\partial x} - \beta\frac{\mu_{a1}}{\mu_1}X_1(a)\right) = \frac{1}{\mu_{\perp 2}}\left(\frac{\partial X_2(a)}{\partial x} - \beta\frac{\mu_{a2}}{\mu_2}X_2(a)\right). \tag{6}$$

The characteristic equation for a ρ value can be obtained by using the Floquet theorem on the MPhC period, namely:

$$\rho X_1(0) = X_2(0 + L),$$

$$\rho\frac{1}{\mu_{\perp 1}}\left(\frac{\partial X_1(0)}{\partial x} - \beta\frac{\mu_{a1}}{\mu_1}X_1(0)\right) = \frac{1}{\mu_{\perp 2}}\left(\frac{\partial X_2(0 + L)}{\partial x} - \beta\frac{\mu_{a2}}{\mu_2}X_2(0 + L)\right). \tag{7}$$

We will find fundamental solutions of the Hill equation as a solution of third boundary value problems with mixed boundary conditions

$$\psi_1(0) = 1, \quad \frac{1}{\mu_{\perp 1}}\left[\frac{\partial\psi_1(0)}{\partial x} - \beta\frac{\mu_{a1}}{\mu_1}\psi_1(0)\right] = 0,$$

$$\psi_2(0) = 0, \quad \frac{1}{\mu_{\perp 1}}\left(\frac{\partial\psi_2(0)}{\partial x} - \beta\frac{\mu_{a1}}{\mu_1}\psi_2(0)\right) = 1.$$

The fundamental solutions of the Hill equation, taking into account the mixed boundary conditions, take the following explicit form for two regions on the period of a one-dimensional MPhC:

$$\psi_1(x) = \begin{cases} \cos\xi_1 x + \beta\frac{\mu_{a1}}{\mu_1}\frac{\sin\xi_1 x}{\xi_1} & 0 < x < a \\ A\cos\xi_2(x - a) + B\frac{\sin\xi_2(x-a)}{\xi_2}, & a < x < L \end{cases}, \tag{8}$$

$$\psi_2(x) = \begin{cases} \mu_{\perp 1}\frac{\sin\xi_1 x}{\xi_1} & 0 < x < a \\ D\cos\xi_2(x - a) + C\frac{\sin\xi_2(x-a)}{\xi_2}, & a < x < L \end{cases}, \tag{9}$$

$$A = \cos\xi_1 a + \beta\frac{\mu_{a1}}{\mu_1}\frac{\sin\xi_1 a}{\xi_1},$$

$$B = \beta\frac{\mu_{a2}}{\mu_2}\cos\xi_1 a - \frac{\mu_{\perp 2}}{\mu_{\perp 1}}\xi_1\sin\xi_1 a + \beta^2\frac{\mu_{a1}}{\mu_1}\left(\frac{\mu_{a2}}{\mu_2} - \frac{\mu_{\perp 2}}{\mu_{\perp 1}}\frac{\mu_{a1}}{\mu_1}\right)\frac{\sin\xi_1 a}{\xi_1},$$

$$C = \mu_{\perp 2}\cos\xi_1 a + \beta\mu_{\perp 1}\left(\frac{\mu_{a2}}{\mu_2} - \frac{\mu_{\perp 2}\mu_{a1}}{\mu_{\perp 1}\mu_1}\right)\frac{\sin\xi_1 a}{\xi_1},$$

$$D = \mu_{\perp 1} \frac{\sin \xi_1 a}{\xi_1}.$$

In addition, it is possible to present the solution of the Hill equation shifted by the period L of the MPhC in explicit form:

$$\begin{pmatrix} \psi_1(x+L) \\ \psi_2(x+L) \end{pmatrix} = \boldsymbol{P} \begin{pmatrix} \psi_1(x) \\ \psi_2(x) \end{pmatrix} = \begin{pmatrix} P_{11} & P_{12} \\ P_{21} & P_{22} \end{pmatrix} \begin{pmatrix} \psi_1(x) \\ \psi_2(x) \end{pmatrix}, \tag{10}$$

$$\boldsymbol{P} = \begin{pmatrix} P_{11} & P_{12} \\ P_{21} & P_{22} \end{pmatrix} = \begin{pmatrix} \psi_1(L) & \frac{1}{\mu_{\perp 2}(L)} \left[\psi_1'(L) - \beta \frac{\mu_{a2}(L)}{\mu_2(L)} \psi_1(L) \right] \\ \psi_2(L) & \frac{1}{\mu_{\perp 2}(L)} \left[\psi_2'(L) - \beta \frac{\mu_{a2}(L)}{\mu_2(L)} \psi_2(L) \right] \end{pmatrix}.$$

To obtain the characteristic equation and determine the Floquet constant ρ, we use Eq. (7). As a result, we obtain:

$$\left(\rho + \rho^*\right) = 2 \cos KL = \frac{1}{\mu_{\perp 2}} \left[\psi_2'(L) - \beta \frac{\mu_{a2}}{\mu_2} \psi_2(L) \right] + \psi_1(L). \tag{11}$$

Using explicit expressions for the fundamental solutions of the Hill Eq. (9) and (10) we obtain an analytical expression for the dispersion equation of a one-dimensional MPhC with gyrotropic layers:

$$\cos K(\beta) L = \cos \xi_2 b \cos \xi_1 a - \frac{1}{2} \left[\frac{\xi_1}{\xi_2} \frac{\mu_{\perp 2}}{\mu_{\perp 1}} + \frac{\xi_2}{\xi_1} \frac{\mu_{\perp 1}}{\mu_{\perp 2}} + \frac{\beta^2}{\xi_1 \xi_2} \frac{\mu_{\perp 2}}{\mu_{\perp 1}} \left(\frac{\mu_{a1}}{\mu_1} - \frac{\mu_{\perp 1}}{\mu_{\perp 2}} \frac{\mu_{a2}}{\mu_2} \right)^2 \right] \sin \xi_2 b \sin \xi_1 a. \tag{12}$$

It should be noted that this dispersion equation completely coincides with the equation obtained using the transfer matrix [3, 6]. Let us proceed to the determination of the coefficients of transmission and reflection of a plane wave for MPhC shown in Fig. 1. We use the boundary conditions for the tangential field components E_z, H_y on two surfaces: $x = 0$ and $x = NL$. Then we obtain matrix equations for determining of the reflection coefficient R_N and transmission one T_N:

$$T_N \begin{pmatrix} 1 \\ i \frac{\xi_{ex}}{\mu_{ex}} \frac{1}{ik} \end{pmatrix} = W^N \begin{pmatrix} 1 + R_N \\ i \frac{\xi_{in}}{\mu_{in}} (1 - R_N) \frac{1}{ik} \end{pmatrix}, \tag{13}$$

where the transfer matrix is defined as:

$$W^N = W \frac{\sin(NKL)}{\sin(KL)} - \vec{1} \frac{\sin[(N-1)KL]}{\sin(KL)}, \tag{14}$$

$$W = \begin{pmatrix} \psi_1(L) & ik \psi_2(L) \\ \frac{1}{ik\mu_{\perp 2}} \left[\psi_1'(L) - \beta \frac{\mu_{a2}}{\mu_2} \psi_1(L) \right] & \frac{1}{\mu_{\perp 2}} \left[\psi_2'(L) - \beta \frac{\mu_{a2}}{\mu_2} \psi_2(L) \right] \end{pmatrix}.$$

The solution of Eq. (13) leads to the following expression for the transmission coefficient T_N, reflection one R_N and power transmission coefficient $|T_N|^2$ for bounded MPhC:

$$T_N = 2\left[\left(W_{22}^N + \frac{\mu_{in}}{\xi_{in}}\frac{\xi_{ex}}{\mu_{ex}}W_{11}^N\right) - \left(\frac{\mu_{in}}{\xi_{in}}kW_{21}^N + \frac{\xi_{ex}}{\mu_{ex}}\frac{1}{k}W_{12}^N\right)\right]^{-1}, \tag{15}$$

$$R_N = 1 - T_N\left(\frac{\mu_{in}}{\xi_{in}}\frac{\xi_{ex}}{\mu_{ex}}W_{11}^N + i\frac{\mu_{in}}{\xi_{in}}W_{21}^N\right). \tag{16}$$

If bounded MPhC is surrounded in front and rear by equal media then one can obtain simplified expression:

$$|T_N|^2 = \left[1 + \sin^2(NKL)\left(\left(\frac{1}{2\sin(KL)}\right)^2\left|\left(\frac{\mu_{in}}{\xi_{in}}kW_{21} + \frac{\xi_{ex}}{\mu_{ex}}\frac{1}{k}W_{12}\right)\right|^2 - 1\right)\right]^{-1}. \tag{17}$$

The minimum values $|T_N|^2_{\min}$ are determined by the expression:

$$|T_N|^2_{\min} = \left[1 + \left(\left(\frac{1}{2\sin(KL)}\right)^2\left|\left(\frac{\mu_{in}}{\xi_{in}}kW_{21} + \frac{\xi_{ex}}{\mu_{ex}}\frac{1}{k}W_{12}\right)\right|^2 - 1\right)\right]^{-1}. \tag{18}$$

If there is no gyrotropy in the layers (dielectric layers), then the expressions written above for the fundamental solutions of the Hill Eq. (8), (9), the dispersion Eq. (12), the transmission and reflection coefficients pass into the well-known expressions [15–23].

3 Analysis of Results

In the general case the propagation features of electromagnetic waves in an MPhCs depend on the Floquet-Bloch wave number and transverse wave numbers ξ_j in each layer. Transverse wave numbers in the absence of losses can be either real or purely imaginary. At real values of ξ_j bulk waves propagate in the MPhCs layers and imaginary values of ξ_j correspond to surface wave modes. Combinations of these modes in different layers are also possible. Real values of K_{TM} correspond to Floquet-Bloch waves propagating in the crystal under the condition $|cosK_{TM}L| \leq 1$ (transmission zones of MPhC). Complex values of Floquet-Bloch wave number correspond to damped waves that are in forbidden zones. The boundaries of the forbidden (transmission) zones are determined by equality $|cosK_{TM}L| = 1$.

Figure 2 shows the dispersion diagrams based on the solutions of Eq. (12) for the case $\mu_{a2} = 0$, where one layer of the magnetophotonic crystal is ferrite and the other layer is a magnetodielectric. The diagrams are projections of a function $K(k, \beta)$ onto the parameter plane (k, β) in a three-dimensional space of wave numbers. The shaded areas correspond to the transmission bands, and the unshaded areas correspond to the forbidden zones. The dispersion diagrams are plotted for the following parameters of the problem: $a = b = 0.5L$, $\varepsilon_1 = \varepsilon_2 = 1$, $\mu_2 = 2$, $\mu_1 = 6$. The dotted line is defined by the straight line $\beta = k\sqrt{\varepsilon_2\mu_2}$, the dash-dotted line is defined by straight line $\beta = k\sqrt{\varepsilon_1\mu_1}$. The diagonal dashed line $k = \beta$ in the figures corresponds to the condition that the phase velocity of the wave equals the velocity of light. Above this light line, the region of the existence of fast space waves is situated, and below the light line, the domain of the existence of damped waves is placed. To identify the features of the wave propagation in such structures, it is necessary to distinguish two cases for the different values of the magnetic field H_0(parameter μ_{a1}), corresponding to the conditions $\mu_{\perp 1} > 0$ and $\mu_{\perp 1} < 0$. An analysis of the solutions of Eq. (12) shows that the number of the transmission bands and band gaps depends on the permittivity of each layer. The solutions of Eq. (12), corresponding to fast waves, are in the regions $k^2\varepsilon_2\mu_2 > \beta^2$ and $k^2\varepsilon_1\mu_1 > \beta^2$ for the corresponding layer. To determine the regions of solutions corresponding to slow waves, the signs in these conditions should be reversed. Various combinations of these regimes are also possible. The presence of gyrotropy in one of the layers (for instance, $\mu_{a1} \neq 0$) allows to control the width of the transmission bands (or band gaps), their location and number within a given frequency range. If the effective permeability of ferrite $\mu_{\perp 1} < 0$, then there is a slowed surface ferrite wave propagating along the interface of two adjacent layers of the structure.

From the solution of the dispersion equation and the form of the fields spatial distribution, it follows that the forward ($\beta = +\mathrm{Re}|\beta|$) and backward ($\beta = -\mathrm{Re}|\beta|$) waves propagating along the layers (the Oy-axis), have the same propagation velocity but different transverse field structure (along the Ox-axis in the crystal). The dispersion diagram in Fig. 2 corresponds to the negative values of effective permeability $\mu_{\perp 1}$. Figure 2 shows four variants of the diagram for the values $\mu_{a1} > 6$.

In the case of the absence of gyrotropy ($\mu_{a1} = 0$, $\mu_2 = 2$, $\mu_1 = 6$) the straight lines $k\sqrt{2} = \beta$ and $k\sqrt{6} = \beta$ determine speed of light inside the magnetodielectric layers. The cases of excitation of both bulk and surface waves inside the layers of the periodic structure are possible. In the presence of the ferrite layer (for $\mu_{a1} = 3$), its effective permeability $\mu_{\perp 1}$ begins to decrease, that leads to a narrowing of the transmission bands, with the simultaneous expansion of the band gaps. A different situation is observed for the negative values of the effective magnetic permeability $\mu_{\perp 1} < 0$ (Fig. 2). In the case $\mu_{a1} = 6.6$ there is one transmission band. Inside the different regions of this band, separated by a light line $k = \beta$, there can exist fast and slow bulk waves. Inside the region of slow waves, their phase velocity v is greater than the phase velocity in the dielectric layer $v = \beta/\left(k\sqrt{2}\right)$, corresponding to the dash-dotted line. As the magnetic field H_0 increases (an increase in the value of μ_{a1}), two transmission bands appear. One of them corresponds to the bulk waves (fast or slow), and the second one corresponds to the surface slow waves (the entire transmission band is at values $v < \beta/\left(k\sqrt{6}\right)$).

The field distribution for such a wave has maximum amplitude at the boundaries of the regions. Inside the ferrite layer, there is a surface wave that propagates along the layer, at its ferrite-dielectric interface, within each period of the structure. Moreover, an analysis of the spatial distribution of the field (along the Ox-axis) for the forward $\beta = +|\beta|$ and backward $\beta = -|\beta|$ surface waves shows that their structure is different. From Fig. 2 it follows that as the value of parameter μ_{a1} increases, a ferrite surface wave appears in the layer ($\mu_{\perp 1} < 0$). When the value of parameter μ_{a1} increases, the region

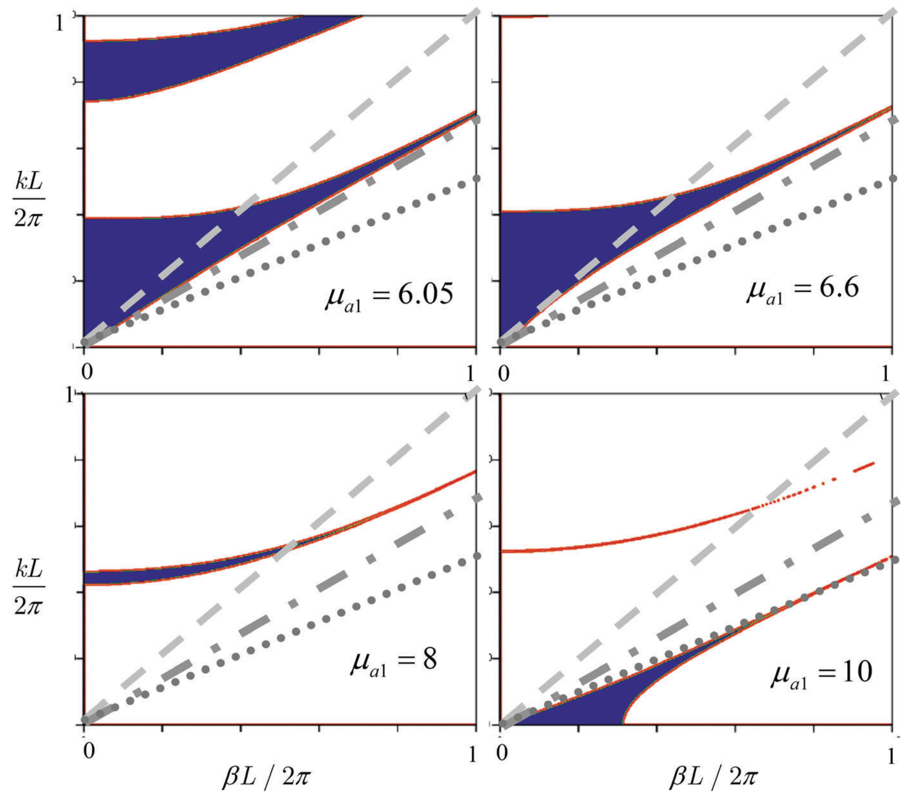

Fig. 2. Dispersion diagrams of magnetophotonic crystal

of the existence of the surface ferrite wave narrows, with the simultaneous contraction of the bulk wave propagation region (case $k\sqrt{2} > \beta$).

Figure 3a shows the dispersion diagram for the MPhC with such parameters values: $N = 5$; $a = 0.2L$; $\mu_1 = 13.8$; $\mu_2 = 3.5$; $\mu_{a1} = 13.7$; $\mu_{a2} = 0$. In this case positive value $\mu_{\perp 1} > 0$ realizes in first layer. Shaded and unshaded areas show transmission zones and forbidden ones respectively.

Figure 3b shows the dependence of the transmission coefficient on the normalized frequency for the case of a normal wave incidence on the MPhC ($\beta = 0$). The dotted curve shows the $|T_N|^2_{\min}$ frequency dependence. It is clear that $(N - 1)$ resonances are observed in the pass-bands.

Figure 4a shows the dispersion diagram for a negative value of effective permeability $\mu_{\perp 1}$ ($\mu_{a1} = 22$). Consequently external magnetic field changing leads to significant changes in the width and location of the pass-bands and the band gaps. This is illustrated in Fig. 4b. Here three transmission zones with different widths are implemented in accordance with the dispersion diagram ($\beta = 0$). It should be noted that four transmission resonances are realized in each pass-band. The quality of resonances increases with decreasing of bandwidth. Figure 5 illustrates this fact. The inset in the Fig. 5 shows the

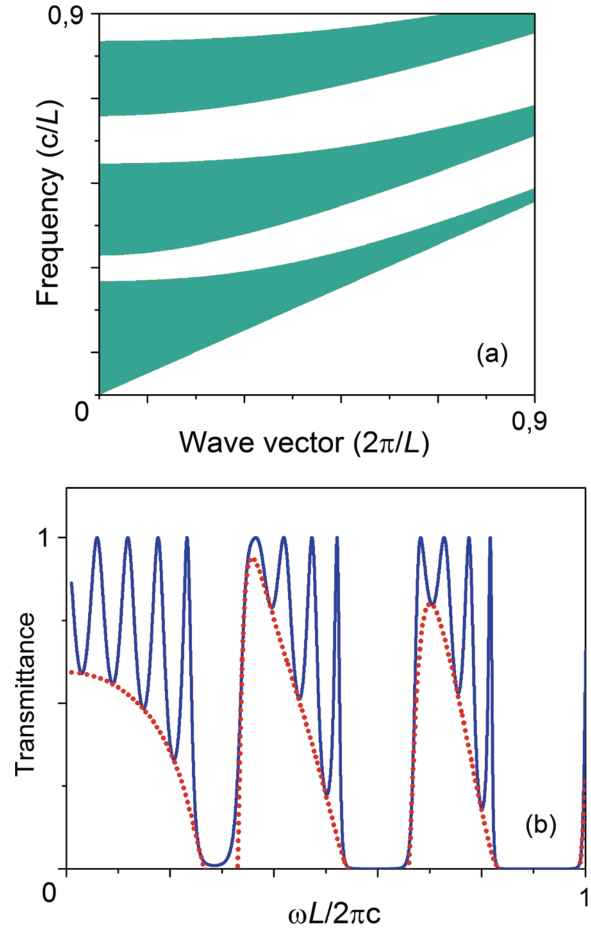

Fig. 3. Dispersion diagram of the infinite magnetophotonic crystal and transmittance of the finite one (5 periods structure)

shape of the resonance marked with a red arrow. It is obvious that in this case additional narrow forbidden zones are realized between the transmission resonances.

The essential advantage of the theory developed by us is the presence of analytical expressions for the spatial distribution of fields in the MPhC layers. These field distributions are determined through the fundamental solutions (8) and (9) of the Hill Eq. (3). Examples of calculations of the electric field distribution within a limited MPhC are presented in Fig. 6. Figure 6a corresponds to the transmission zone in Fig. 3 for the value of the normalized frequency $\omega L/2\pi c = 0.521$ (transmission resonance). Figure 6b corresponds to the forbidden zone in Fig. 4 for the value of the normalized frequency $\omega L/2\pi c = 0.28$. It is obvious that Fig. 6a shows the mode of the bounded MPhC at the resonant frequency. Field intensity maximum realizes at the center of MPhC. The distribution of the electric field in the forbidden zone is characterized by amplitude attenuation during wave propagation through the MPhC.

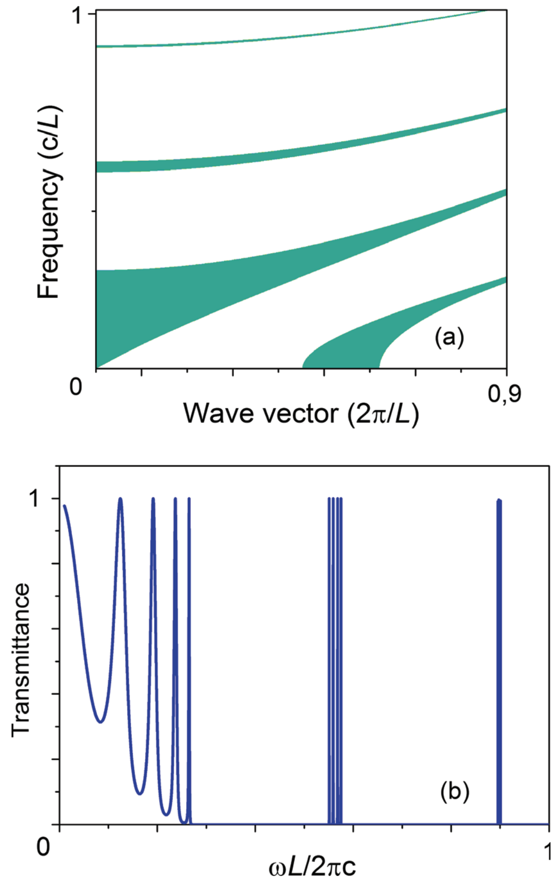

Fig. 4. Dispersion diagram of the infinite magnetophotonic crystal and transmittance of the finite one (5 periods structure)

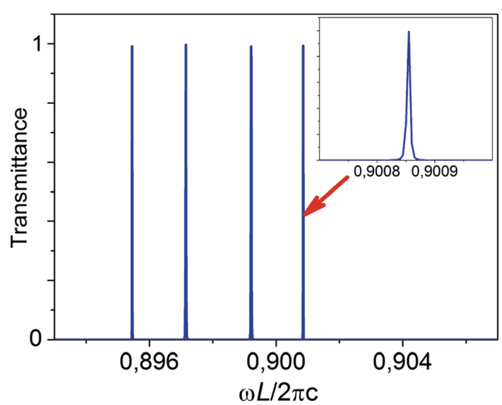

Fig. 5. Transmittance vs normalized frequency for high frequency transmission band in Fig. 4

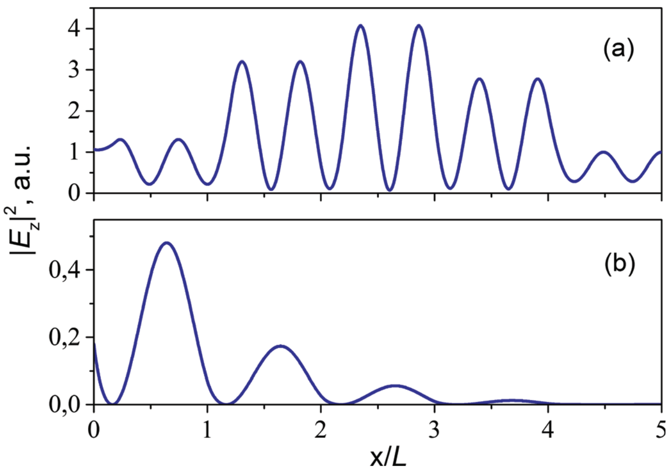

Fig. 6. Spatial distributions of electric field within finite magnetophotonic crystal; (a) – frequency lies in transmission band; (b) – frequency corresponds to band gap

4 Conclusions

The developed Floquet analytic theory for determining eigenfunctions, dispersion characteristics, reflection coefficients and transmission ones of TM waves through a one-dimensional MPhC with arbitrary material parameters of the gyrotropic layers makes it possible to construct a theory of controlled waveguide structures, the surfaces of which can be Bragg reflecting surfaces. An alternative approach based on the use of mixed boundary conditions for the Hill equation allows obtaining analytical expressions for fundamental solutions, dispersion equation and spatial distributions of the magnetic component of the electromagnetic field in MPhC.

In addition, tunable MPhC can be used as controlled deceleration systems in novel terahertz oscillators and amplifiers [24–28].

References

1. Bass, F.G., Bulgakov, A.A.: Kinetic and Electrodynamic Phenomena in Classical and Quantum Semiconductor. Nova Science Publishers, New York (1997)
2. Sakaguchi, S., Sugimoto, N.: Transmission properties of multilayer films composed of magneto-optical and dielectric materials. J. Lightwave Technol. **17**(6), 1087–1092 (1999)
3. Shmat'ko, A.A., Mizernik, V.N., Odarenko, E.N., Yampol'skii, V.A., Rokhmanova, T.N., Galenko, A.Yu.: Dispersion properties of a one-dimensional anisotropic magnetophotonic crystal with a gyrotropic layer. In: 7th International Proceedings on Advanced Optoelectronics and Lasers (CAOL 2016), Odessa, Ukraine, pp. 126–128. IEEE (2016)
4. Shramkova, O.V.: Transmission properties of ferrite-semiconductor periodic structure. Progress Electromagn. Res. **7**, 71–85 (2009)
5. Fu, J.X., Liu, R.J., Li, Z.Y.: Experimental demonstration of tunable gyromagnetic photonic crystals controlled by dc magnetic fields. EPL **89**, 64003 (2010)

6. Shmat'ko, A.A., Mizernik, V.N., Odarenko, E.N., Lysytsya, V.T.: Dispersion properties of TM and TE modes of gyrotropicmagnetophotonic crystals. In: Vakhrushev, A. (ed.) Theoretical Foundations and Applications of Photonic Crystals. InTech (2018)
7. Lyubchanskii, I.L., Dadoenkova, N.N., Lyubchanskii, M.I., Shapovalov, E.A.: Magnetic photonic crystals. J. Phys. D Appl. Phys. **36**, 277–287 (2003)
8. Inoue, M., Fujikawa, R., Baryshev, A., Khanikaev, A., Lim, P.B., Uchida, H., et al.: Magnetophotonic crystals. J. Phys. D Appl. Phys. **39**, 151–161 (2006)
9. Stoker, J.J.: Nonlinear Vibrations. Interscience Publishers, New York (1950)
10. Yakubovich, V.A., Starzhinskii, V.M.: Linear Differential Equations with Periodic Coefficients. Wiley, New York (1975)
11. Eastham, M.S.P.: The Spectral Theory of Periodic Differential Equations. Scottish Academic Press, Edinburgh and London (1973)
12. Magnus, W., Winkler, S.: Hill's Equation. Dover Publications, Mineola (2004)
13. Gurevich, A.G.: Ferrites at Microwave Frequencies. Consultans Bureau, New York (1963)
14. Yeh, P., Yariv, A., Hong, C.: Electromagnetic propagation in periodic stratified media. I. General theory. J. Opt. Soc. Am. **67**(4), 423–438 (1977)
15. Sprung, D.W.L., Wu, H., Martorell, J.: Scattering by a finite periodic potential. Am. J. Phys. **61**, 1118–1124 (1993)
16. Vezzetti, D.J., Cahay, M.M.: Transmission resonances in finite, repeated structures. J. Phys. D Appl. Phys. **19**, L53–L55 (1986)
17. Lekner, J.: Light in periodically stratified media. J. Opt. Soc. Am. A **11**, 2892–2899 (1994)
18. Nusinsky, I., Hardy, A.A.: Band-gap analysis of one-dimensional photonic crystals and conditions for gap closing. Phys. Rev. B. **73**, 125104 (2006)
19. Nurligareev, J.K., Sychugov, V.A.: Propagation of light in a one-dimensional photonic crystal: analysis by the Floquet-Bloch function method. Quantum Electron. **38**, 452–461 (2008)
20. Morozov, G.V., Sprung, D.W.L.: Floquet-Bloch waves in one-dimensional photonic crystals. EPL **96**, 54005 (2011)
21. Nurligareev, J.K.: Floquet-Bloch waves in bound one dimensional photonic crystals. J. Surf. Invest. **5**, 193–208 (2011)
22. Morozov, G.V., Sprung, D.W.L.: Transverse-magnetic-polarized Floquet-Bloch waves in one-dimensional photonic crystals. J. Opt. Soc. Am. B **29**, 3231–3239 (2012)
23. Morozov, G.V., Sprung, D.W.L.: Band structure analysis of an analytically solvable Hill equation with continuous potential. J. Opt. **17**, 035607 (2015)
24. Odarenko, E.N., Shmat'ko, A.A.: Novel THz sources with profiled focusing field and photonic crystal electrodynamic systems. In: International Proceedings on Modern Problems of Radio Engineering, Telecommucations, and Computer Science (TCSET 2016), pp. 345–347. IEEE, Lviv-Slavsko, Ukraine (2016)
25. Odarenko, E.N., Sashkova, Y.V., Shmat'ko, A.A., Shevchenko N.G.: Analysis of slow wave modes in modified photonic crystal waveguides using the MPB package. In: International Proceedings on Mathematical Methods in Electromagnetic Theory (MMET 2018), Kyiv, Ukraine, pp. 164–167. IEEE (2018)
26. Shmat'ko, A.A., Mizernik, V.N., Odarenko, E.N.: Surface and bulk modes of magnetophotonic crystals. In: 14th International Proceedings on Advanced Trends in Radio Electronics, Telecommunications and Computer Engineering (TCSET 2018), Lviv-Slavsko, Ukraine, pp. 436–440. IEEE (2018)
27. Odarenko, E.N., Sashkova, Y.V., Shmat'ko, A.A.: Localized field enhancement in slow-wave modes of modified Bragg waveguide. In: International Proceedings on Microwaves, Radar and Remote Sensing Symposium (MRRS 2017), Kyiv, Ukraine, pp. 147–150. IEEE (2017)
28. Odarenko, E.N., Shmat'ko, A.A.: Photonic crystal and Bragg waveguides for THz electron devices. In: 13th International Proceedings on Laser and Fiber-Optical Networks Modeling (LFNM 2016), Odesa, Ukraine, pp. 53–55. IEEE (2016)